



HAL
open science

Vanadium-Catalyzed Terpolymerization of α,ω -Dienes with Ethylene and Cyclic Olefins: Ready Access to Polar-Functionalized Polyolefins

Benedetta Palucci, Giorgia Zanchin, Giovanni Ricci, Laure Vendier, Christian Lorber, Giuseppe Leone

► **To cite this version:**

Benedetta Palucci, Giorgia Zanchin, Giovanni Ricci, Laure Vendier, Christian Lorber, et al.. Vanadium-Catalyzed Terpolymerization of α,ω -Dienes with Ethylene and Cyclic Olefins: Ready Access to Polar-Functionalized Polyolefins. *Macromolecules*, 2021, 54 (23), pp.10700-10711. 10.1021/acs.macromol.1c02142 . hal-03518735

HAL Id: hal-03518735

<https://hal.science/hal-03518735v1>

Submitted on 14 Oct 2022

HAL is a multi-disciplinary open access archive for the deposit and dissemination of scientific research documents, whether they are published or not. The documents may come from teaching and research institutions in France or abroad, or from public or private research centers.

L'archive ouverte pluridisciplinaire **HAL**, est destinée au dépôt et à la diffusion de documents scientifiques de niveau recherche, publiés ou non, émanant des établissements d'enseignement et de recherche français ou étrangers, des laboratoires publics ou privés.

Vanadium–Catalyzed Terpolymerization of α,ω -Dienes with Ethylene and Cyclic Olefins: Ready Access to Polar–Functionalized Polyolefins

Benedetta Palucci,[†] Giorgia Zanchin,[†] Giovanni Ricci,[†] Laure Vendier,^{l,#}
Christian Lorber^{l,#} and Giuseppe Leone^{†,*}

[†] CNR-Istituto di Scienze e Tecnologie Chimiche “Giulio Natta” (SCITEC), via A. Corti 12, I-20133 Milano, Italy.

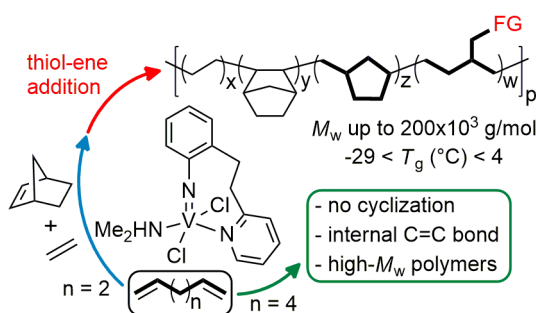
^l CNRS, LCC (Laboratoire de Chimie de Coordination), 205 route de Narbonne, BP44099, 31077 Toulouse, France

[#] Université de Toulouse, UPS, INPT, LCC, 31077 Toulouse, France

* Corresponding author: giuseppe.leone@scitec.cnr.it

Keywords: vanadium; functionalized polyolefins; nonconjugated dienes; ring closure; thiol-ene addition

For Table of Contents use only



Abstract. α,ω -Dienes are an important class of (co)monomers due to their utility in the synthesis of cyclopolyolefins and *reactive polyolefin intermediates*. In this contribution, the terpolymerization of two α,ω -dienes (*i.e.*, 1,5-hexadiene and 1,7-octadiene) with ethylene and various cyclic olefins [*i.e.*, norbornene (NB), 5-ethylidene-2-norbornene (ENB) and dicyclopentadiene (DCPD)] catalyzed by a chelated imido vanadium complex has been examined. The ENB and DCPD diene termonomers provide additional sites for post-polymerization functionalization. Vanadium–catalyzed terpolymerization of the investigated α,ω -dienes yields polyolefins with high molecular weight (M_w up to 200×10^3 g mol⁻¹), unimodal and narrow molecular weight distribution, sub-ambient glass

transition temperatures ($-30 < T_g \text{ } ^\circ\text{C} < -3$) and a proper content of C=C bonds. Comprehensive NMR investigation of the obtained polymers revealed that subtle changes in the α,ω -diene size have important effects on the numerous combinations of insertion paths (ring closure *vs* ring opening) from which different repeating units with a C=C bond in the side or main polymer chain and cyclic units are installed. Finally, the poly(ethylene-*ter*-1,5-hexadiene-*ter*-NB) was subjected to thiol-ene addition using thioglycolic acid, methyl thioglycolate and *N*-acetyl-L-cysteine to access polar functionalized polyolefins with degree of functionalization and properties dependent on the thiol substitution.

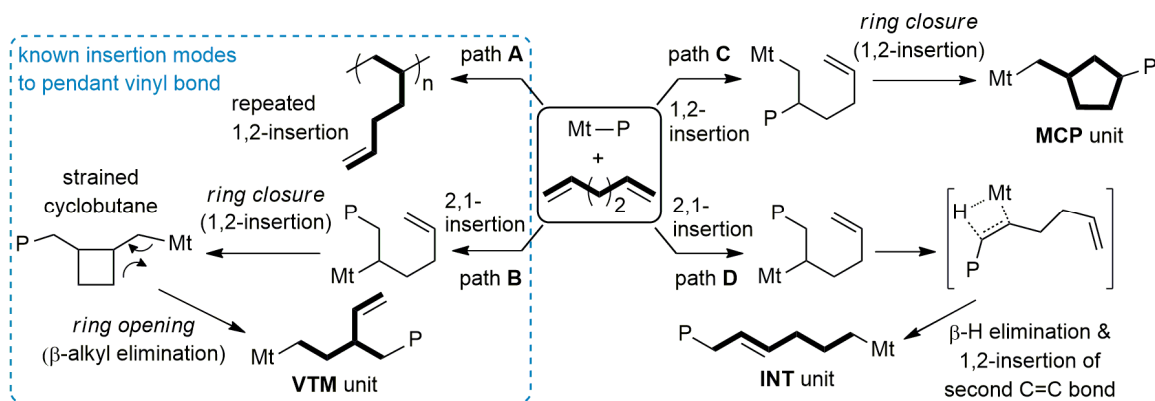
INTRODUCTION

Coordination–insertion (co)polymerization of olefins mediated by transition metal catalysts is among the largest scale synthetic chemical transformation that enables the synthesis of high molecular weight (MW) polyolefins.^{1–5} Polyolefins have become prominent in the marketplace: they excel in chemical and mechanical properties, energy efficiency, are economically and ecologically attractive materials, and continue to experience an ever-growing demand in a myriad of applications.^{6–9} Nonetheless, polyolefins are hydrophobic and their application in blending, adhesion and dyeing remain difficult due to a lack of functional groups. Therefore, the synthesis of specialty polyolefins with unsaturated reactive groups and functionality is a key target.^{10–12} It is expected that the direct introduction of a few percent of functional groups may enlarge the scope of polyolefins to construct engineering materials. In this respect, the insertion (co)polymerization of olefins with polar (co)monomers,^{13–15} and the post–polymerization modification is a highly sought-after area of research.^{16–19} Polyolefins having pendant C=C groups are valuable and promising candidates: the modification of *reactive polyolefin intermediates* is a profitable and easy alternative to the copolymerization of polar monomers. It exploits the reactivity of double bonds, including thiol–ene ligations, epoxidation and hydrosilylation.^{20–25}

The (co)polymerization of nonconjugated dienes may be a convenient and straightforward way to synthesize *reactive polyolefin intermediates*. Indeed, 1,2- (or 2,1-) insertions of an α,ω -diene install an alkyl branch with a terminal C=C bond in the repeating unit (Scheme 1, path A). Pendant vinyl groups may be also formed through a 2,1-insertion, subsequent 1,2-insertion of the remaining C=C bond (*ring closure*) to give, for example in the case of 1,5-hexadiene, a strained cyclobutane ring followed by β -alkyl activation (*ring opening* - Scheme 1, path B).²⁶ The result of this mechanism is the placement of a 3-vinyl-tetramethylene unit (referred to “VTM”). However, it is documented that the polymerization of α,ω -dienes often faces many difficulties to yield polymers with pendant vinyl moieties due to a more favorable 1,2-insertion and subsequent cyclization by 1,2-insertion of the second C=C bond [*i.e.*, methylene-1,3-cyclopentane (MCP) for 1,5-hexadiene (Scheme 1, path

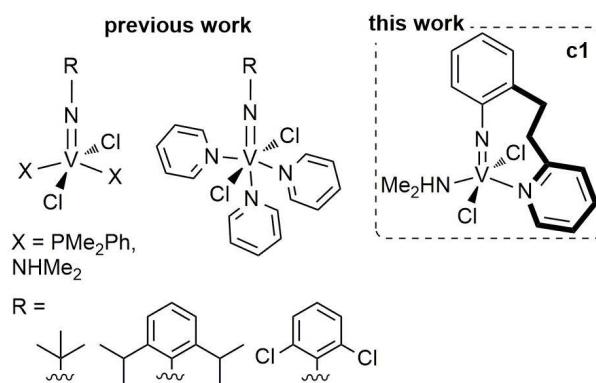
C)].²⁶ Moreover, the insertion polymerization of α,ω -dienes has many limitations such as a significant decrease in productivity and MW, which is critical to ensure satisfactory polymer tensile properties.

Scheme 1. Known insertion modes of α,ω -dienes. The example of 1,5-hexadiene.



So far, the homopolymerization of α,ω -dienes has been extensively investigated using Ti, Zr, Hf, Sc, Co and Fe based catalysts.²⁷ By contrast, examples of α,ω -diene copolymerization are scarce,^{28–31} while terpolymerization of nonconjugated dienes with olefins is largely unexplored likely because nonconjugated dienes and simple olefins often show unmatched reactivity and give, in some cases, a mixture of homopolymers.³² Notably, it is challenging to achieve (co)polymers with good diene incorporation while maintaining high productivity, high-MW, and avoiding irreversible permanent cross-linking that negatively affects the material processing and properties. Successful examples of terpolymerization of α,ω -dienes with ethylene and styrene were reported by Hou *et al.*,^{33,34} and Nomura *et al.*³⁵ by using half-sandwich Sc complexes and aryloxo-modified half-titanocenes, respectively. Conversely, while the utilization of vanadium catalysts in simple olefin (co)polymerization has been extensively studied,³⁶ few examples of vanadium catalysts promoting the polymerization of α,ω -dienes have been reported. These include $V(\text{acac})_3$ in combination with Et_2AlCl .^{37,38} Previously, we reported a series of imido V(IV) precatalysts, which promote the copolymerization of ethylene with α -olefins,³⁹ and cyclic olefins to afford thermoplastics and polyolefin elastomers (Chart 1).^{40,41} Further investigations on these complexes revealed that changing the imido skeleton significantly affects the catalytic performance.

Chart 1. Imido V(IV) complexes previously reported by our group, and **c1** synthesized in this work.



In this study, we describe the synthesis of a chelated imido V(IV) precatalyst (**c1** - Chart 1) and its catalytic behavior in the terpolymerization of α,ω -dienes (*i.e.*, 1,5-hexadiene and 1,7-octadiene) with ethylene and cyclic olefins [*i.e.*, norbornene (NB), 5-ethylidene-2-norbornene (ENB) and dicyclopentadiene (DCPD)]. We postulate that **c1** would have beneficial effects in slowing the rate of β -H elimination and subsequent chain transfer since the coordinating nitrogen atoms of the imido and pyridine moieties are expected to be always *cis* to one another, and hence forcing the growing polymer chain and the last inserted monomer unit in *cis* position as well, which is the most favorable situation for chain growth.⁴² Soluble polymers with a favorable content of unsaturated reactive groups, high-MW (up to $200 \times 10^3 \text{ g mol}^{-1}$) and subambient glass transition temperatures ($-30 < T_g \text{ } ^\circ\text{C} < -3$) were successfully obtained. As a proof of concept, the poly(ethylene-*ter*-1,5-hexadiene-*ter*-norbornene) was subjected to further thiol-ene addition by using thioglycolic acid, methyl thioglycolate and *N*-acetyl-L-cysteine to access polar-functionalized polyolefins.

Results and Discussion

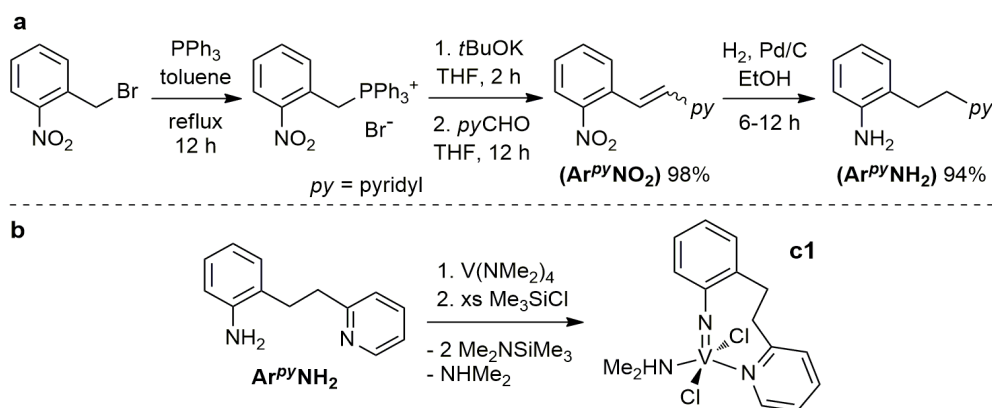
Synthesis and Characterization of **c1**.

The pyridine-aniline proligand Ar^{py}NH₂ was prepared following an analogous procedure developed for the synthesis of other anilines with pendant *ortho*-substituents employed in chelating imido Ti compounds.⁴³ The ligand is obtained in good yield by a three-step synthesis (Scheme 2a). The procedure starts from 2-nitro-benzyl bromide to give Ar^{py}NH₂ with a two carbon atoms linker between the aniline and the pyridyl pendant group. Successively, two different synthetic routes were

attempted to achieve the complexation of $\text{Ar}^{\text{py}}\text{NH}_2$ and to form the desired complex. The first one was an imido exchange transamination-type reaction between the imido precursor $\text{V}(=\text{N}-t\text{Bu})\text{Cl}_2(\text{NHMe}_2)_2$ and $\text{Ar}^{\text{py}}\text{NH}_2$ (Scheme S1), a typical reaction commonly used in the analogue titanium chemistry to generate aryl-imido or hydrazido compounds,^{44–47} while the second route was a transamination reaction from the amido precursor $\text{V}(\text{NMe}_2)_4$ in the presence of Me_3SiCl (Scheme 2b),^{48,49} successfully used to synthesize various Ti and V compounds with different imido functions.^{45,50–55} The first synthetic route proved to be unsuccessful in the production of the desired imido complex. Indeed, the stoichiometric reaction between $\text{V}(=\text{N}-t\text{Bu})\text{Cl}_2(\text{NHMe}_2)_2$ and $\text{Ar}^{\text{py}}\text{NH}_2$ in toluene shows no sign of transformation at room temperature (the solution remains green), while after heating overnight at 90 °C the solution turned red-orange. An EPR study of the crude solution showed the presence of several species (Figure S1). Selective crystallization afforded three crops of crystals. The first green crystals were shown by an X-ray diffraction study to be the $\text{Ar}^{\text{py}}\text{NH}_2$ adduct [*i.e.*, $[\text{V}(=\text{N}-t\text{Bu})\text{Cl}_2(\text{Ar}^{\text{py}}\text{NH}_2)]_2$ (**a1**) – Figure S2], while recording the cell parameters of the blue-green crystals obtained in the second crop proved this compound to be the starting imido complex $\text{V}(=\text{N}-t\text{Bu})\text{Cl}_2(\text{NHMe}_2)_2$ which structure is known.³⁹ The third crop afforded a mixture of colorless and red crystals of so far unknown composition.

On the contrary, the transamination reaction between $\text{V}(\text{NMe}_2)_4$ and $\text{Ar}^{\text{py}}\text{NH}_2$ in excess Me_3SiCl in toluene, at room temperature, produced the desired imido complex $\text{V}(=\text{N}-\text{Ar}^{\text{py}})\text{Cl}_2(\text{NHMe}_2)$ (**c1**) as a pale orange solid, in good yield (Scheme 2b). Differently to the case of some titanium complexes with similar imido ligands having a pendant donor group (with O, N, S donors),⁴³ in this case we did not observe the formation of vanadium intermediates with two dimethylamine ligands and uncoordinated pyridinic nitrogen atom.

Scheme 2. Synthetic method used to prepare (a) $\text{Ar}^{\text{py}}\text{NH}_2$ proligand, and (b) **c1**.



Due to its electronic d^1 configuration, **c1** is NMR silent (^1H , ^{51}V) but EPR active (Figure S3). Its EPR spectrum consists of an eight-line pattern with $g_{\text{iso}} = ca. 1.9855$, and $A_{\text{iso}}(^{51}\text{V}) = 93 \text{ G}$, in agreement to previously reported examples of imido V(IV) complexes ($I = 7/2$ for ^{51}V).⁴⁷ Crystals suitable for crystal structure determination were obtained for **c1**, which allows to unequivocally confirm its structure and enables a direct comparison with other known structures of similar complexes such as the representative examples $\text{V(=N-}^t\text{Bu)Cl}_2(\text{NHMe}_2)_2$,³⁹ $\text{V(=N-2,6-}^i\text{Pr}_2\text{-C}_6\text{H}_3\text{)Cl}_2(\text{Py})_3$,^{48,49} and $\text{V(=N-2,6-}^i\text{Pr}_2\text{-C}_6\text{H}_3\text{)Cl}_2(\text{NHMe}_2)_2$.⁴⁹ An ORTEP drawing of **c1** is displayed in Figure 1, while Figure 2 presents two different views of the structure to better assess the chelating ligand arrangement. Crystallographic data and important metric parameters are summarized in Table S1 and S2.

Complex **c1** shares structural features with the known parents $\text{V(=N-R)Cl}_2(\text{NHMe}_2)_2$,^{39,48,49} and also to the imido chelate titanium congeners $[\text{Ti(=N-Ar}^{\text{PG}}\text{)Cl}_2(\text{NHMe}_2)]$.⁴³ The pentacoordinated vanadium center adopts a distorted square pyramidal geometry with the imido group in apical position as reflected by the measure of the τ parameter ($\tau = 0.29$).⁵⁶ The salient bond parameters are typical of such imido complexes: a short V–N bond distance of $1.656(2) \text{ \AA}$ with an almost linear V–N–C imido linkage ($168.5(2)^\circ$). The dimethylamino ligand is in *trans* position to the pyridine group [$\text{NH-V-N}_{\text{Py}} = 157.88(9)^\circ$], with V–NH and V–N_{Py} of $2.145(2) \text{ \AA}$ and of $2.174(2) \text{ \AA}$, respectively. The two mutually *cis* chlorine atoms have mean V–Cl bonds of *ca* 2.33 \AA , and Cl–V–Cl angle = *ca.* 141° .

Figure 1. Molecular structure of **c1**. Thermal ellipsoids are drawn at the 50% probability level and partial atom-labeling schemes. Hydrogen atoms are omitted for clarity (except for H atoms on the dimethylamino ligand).

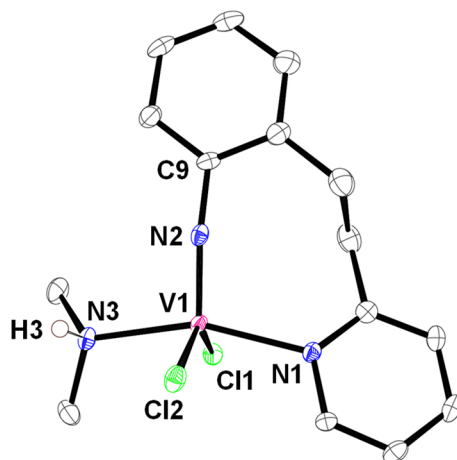
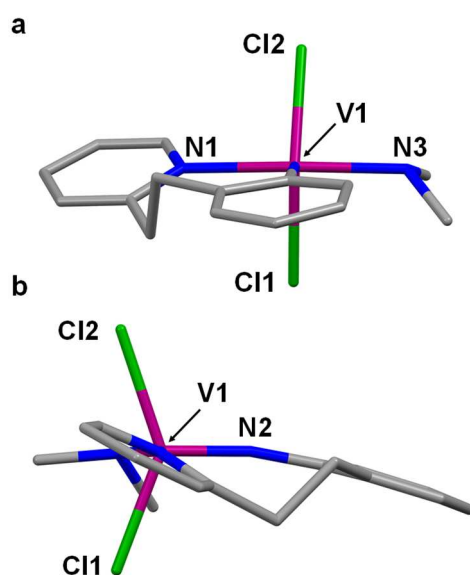
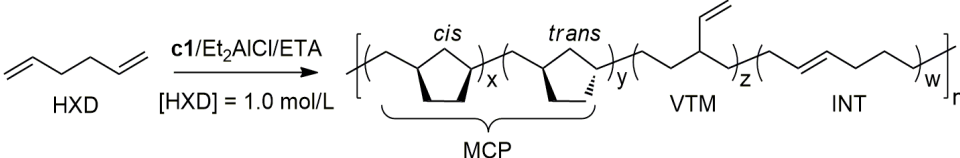


Figure 2. Two different views of the molecular structure of **c1**: (a) along the C–N–V imido bond, and (b) along the N^{py} –V bond.



Homopolymerization of 1,5-hexadiene and 1,7-octadiene. The catalytic utility of **c1** was first investigated in the homopolymerization of 1,5-hexadiene and 1,7-octadiene using Et_2AlCl as the cocatalyst (500 equiv. to V) and in the presence of ethyltrichloroacetate (ETA, 10 equiv. to V), which acts as reoxidant.⁵⁷ Some representative results are summarized in Table 1.

Table 1. Homopolymerization of 1,5-Hexadiene (HXD) and 1,7-Octadiene (OTD) Using **c1**/Et₂AlCl/ETA.^a



entry	α,ω -diene	yield		$M_w^b \times 10^3$ (g/mol)	M_w/M_n^b	enchainment type (mol%) ^c			T_g^d (°C)
		(g)	(%)			MCP (cis/trans)	VTM	INT	
1	HXD	0.41	27	47	2.3	50.7 (41/59)	45.5	3.8	-17
2	OTD	na							

^a polymerization conditions: total volume, 18 mL (toluene); **c1**, 5 μ mol; Al/V = 500; ETA/V = 10; [diene] = 1.0 mol/L; time, 5h; temperature, 20 °C; ^b determined by SEC; ^c determined by NMR; ^d determined by DSC (second heating); na, no solid polymer was recovered.

The homopolymerization of 1,5-hexadiene formed a soluble, solid polymer with M_w of 47×10^3 g mol⁻¹, rather narrow molecular weight distribution ($M_w/M_n = 2.3$) and a T_g of -17 °C. The polymer characterization by ¹H and ¹³C NMR revealed a high degree of unsaturation and the presence of three types of polymer chain fragments: methylene-1,3-cyclopentane units (referred to “MCP”), 3-vinyl-tetramethylene units (referred to “VTM”) and linear C6 segments with an internal C=C bond (referred to “INT”) (Figure S4–S5 and Table S3).²⁸ Overall, NMR data indicate that **c1** exhibits regio-random insertion of 1,5-hexadiene, *i.e.*, it does not have a significant selectivity for 1,2- vs 2,1-insertion. The polymer consists of 50.7 mol% MCP, the *trans* configuration being slightly prevalent, 45.4 mol% VTM and 3.8 mol% INT unit. The presence of MCP and VTM units may be easily explained by 1,2-insertion followed by intramolecular cyclization (Scheme 1, path C), and 2,1-insertion followed by cyclization and β -alkyl elimination (Scheme 1, path B), respectively. The presence of linear chain fragments with an internal C=C bond indicates that a different insertion path becomes competitive to some extent. This is path D in Scheme 1, an uncommon and rare insertion mode of α,ω -dienes. Path D was first documented by Hasegawa *et al.*,⁵⁸ and, more recently, by Huang *et al.* which found that the formation of such linear segments involves a 2,1-insertion of the first vinyl groups into a Mt–C bond and β -H elimination followed by 1,2-insertion of the remaining C=C group into a Mt–H bond.⁵⁹ To be noted, pendant 3-butenyl group, expected from successive 1,2-insertion

of 1,5-hexadiene (Scheme 1, path A), was not observed: 1,2-insertion is preferentially followed by ring closure that evolves into a MCP unit (Scheme 1, path C).

Conversely, **c1**/Et₂AlCl/ETA exhibited no activity for the polymerization of 1,7-octadiene. No solid polymer was recovered under the conditions employed. The lack of productivity may be due to the more space demanding coordination–insertion of 1,7-octadiene and thus to a higher steric congestion in the coordination plane with negative effects on the insertion of the incoming monomer and chain growth. Faster β–H elimination and subsequent chain transfer may also account for.

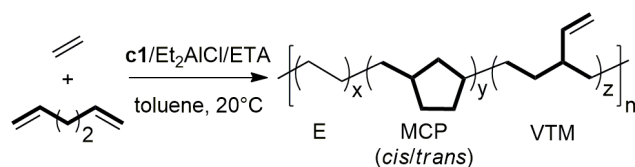
Co- and Ter-polymerization of 1,5-Hexadiene. The copolymerization of 1,5-hexadiene with ethylene was investigated at 1 atm of ethylene, E/HXD feed ratio of 1/4, in a semi-batch mode: the ethylene gaseous monomer was replenished by maintaining a constant pressure over the reaction time course, while the liquid diene was placed in the reactor at the beginning of the reaction (Table 2, entry 3).

Table 2. 1,5-Hexadiene (HXD) Copolymerization and Terpolymerization Studies Using **c1**/Et₂AlCl/ETA. 1-Hexene (HEX) (co)polymerizations are added for comparison.^a

entry	M1	M2	E/M1/M2 ^b	yield (g)	activity ^c	composition (mol%) ^d					$M_w^e \times 10^3$ (g/mol)	M_w/M_n^e	$T_g^f(T_m)$ (°C)
						E	MCP	VTM	HEX	M2			
3	HXD		1/4	0.80	2410	77.9	18.9 ^g	3.2			123	2.7	–24 (53,89)
4	HEX		1/4	0.26	790	91.0			9.0		72	2.2	(78,90)
5	HXD	NB	1/4/0.5	0.86	2565	78.3	6.1	3.2		12.4	158	2.0	–3
6	HXD	ENB	1/4/0.5	0.89	2670	73.1	14.2	4.3		8.4	120	2.5	–5
7 ^h	HEX	ENB	1/4/0.5	0.37	550	88.9			4.8	6.3	51	1.9	–20 (53)
8	HXD	DCPD	1/4/0.5	0.72	2170	80.4	10.7	3.0		5.8	130	1.9	–6 (44)

^a polymerization conditions: ethylene pressure, 1.01 bar; total volume, 50 mL (toluene); **c1**, 5 μmol; Al/V = 500; ETA/V = 10; temperature, 20 °C; time, 4 min; [M1] = 0.56 mol/L; [M2] = 0.07 mol/L; ^b (co)monomer feed ratio (mol/mol) in liquid phase; ^c activity in kg_{pol} × (mol_v × h)^{–1}; ^d determined by NMR; ^e determined by SEC; ^f determined by DSC (second heating); ^g *cis/trans* = 52/48; ^h time, 8 min. Each test was repeated at least 3 times with an error on the yield data of less than 10%.

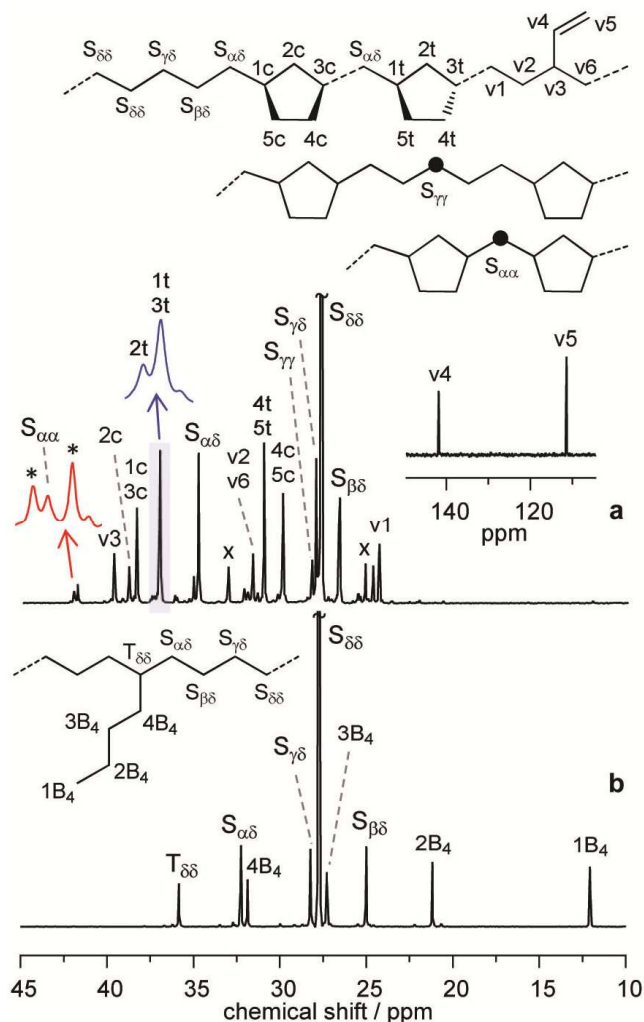
Scheme 3. Copolymerization of ethylene with 1,5-hexadiene by **c1**/Et₂AlCl/ETA.



c1/Et₂AlCl/ETA catalyzed the copolymerization of ethylene with 1,5-hexadiene to give a soluble, solid copolymer with high molecular weight ($M_w = 123 \times 10^3 \text{ g mol}^{-1}$), unimodal molecular weight distribution ($M_w/M_n = 2.7$) and high 1,5-hexadiene incorporation (Table 2, entry 3). The copolymerization exhibited very high initial efficiency and fast monomer consumption, so that the copolymerization was stopped rapidly to keep low the 1,5-hexadiene conversion for preventing cross-linking and to avoid mass transport limitations caused by filling of the reactor with the swollen polymer. Solvent fractionation confirmed that the obtained copolymer does not contain byproduct homopolymers.

The copolymer microstructure was investigated by NMR. Figure 3a shows the whole ¹³C NMR spectrum, and methylene and methine carbons were distinguished by DEPT (Figure S7). In addition to the characteristic peaks of long methylene segments (S₈₈ at 27.7 ppm), the ¹³C NMR spectrum shows the resonances ascribed to *trans* (referred to 1t–5t) and *cis* (referred to 1c–5c) MCP fragments, and those to unsaturated VTM ones (referred to v1–v5, Table S4). NMR analysis established that the copolymer is formed by 77.9 mol% of ethylene, 18.9 mol% MCP, and 3.2 mol% VTM. The presence of ethylene in the copolymerization mixture has a large effect on the 1,5-hexadiene enchainment, MCP units being increasingly predominant in the copolymer. The preference for the formation of MCP over VTM chain fragments indicates that 1,2-insertion of 1,5-hexadiene followed by cyclization (Scheme 1, path C) is favored over 2,1-insertion (Scheme 1, path B). This may be most likely because a 2,1-insertion is much more space demanding.⁶⁰ Note that resonances characteristic of pendant 3-butenyl groups, associated to successive 1,2-insertions of 1,5-hexadiene (Scheme 1, path A), were not detected: the ring closure is even faster than the insertion of ethylene. Likewise, the lack of linear enchainment units with an internal C=C bond suggests that path D does not occur in the presence of ethylene: the 2,1-insertion of 1,5-hexadiene preferentially evolves into methylenecyclobutane intermediate followed by ring opening to yield a VTM unit (Scheme 1, path B).

Figure 3. ^{13}C NMR spectra (in $\text{C}_2\text{D}_2\text{Cl}_4$ at 103°C , reference to HDMS) of (a) entry **3**, and (b) entry **4**. The signals marked with a cross, and an asterisk are difficult to assign definitively. We hypothesized that those marked with a cross are likely due to carbon in α and β position to MCP units in MCP/E/VTM, MCP/E/MCP or MCP/VTM sequences, while those marked with an asterisk are certainly tertiary carbon atoms, as indicated by the DEPT, in MCP/E/VTM, MCP/VTM or, although unlikely, in VTM/VTM sequences.

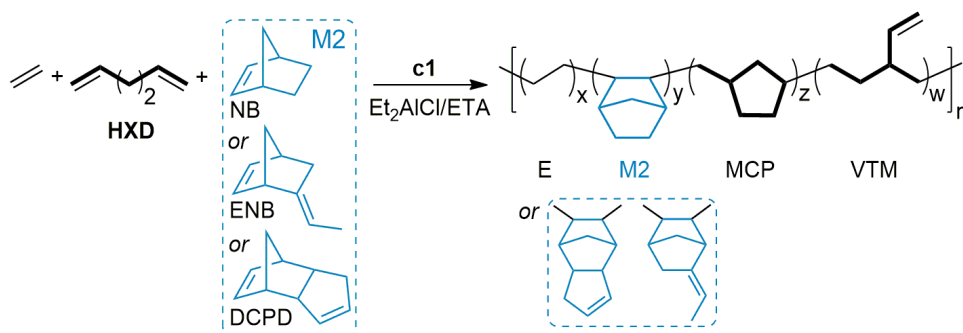


To tentatively explain the effect of the remaining $\text{C}=\text{C}$ bond, the copolymerization of 1-hexene with ethylene was performed under the same reaction conditions (Table 2, entry 4). The ^{13}C NMR spectrum of entry **4** confirmed the formation of the expected random poly(ethylene-*co*-1-hexene) with isolated 1,2-inserted butyl branches (Figure 3b).⁶¹ Compared to the same experiment with 1,5-hexadiene, the addition of 1-hexene was detrimental to the activity and led to more than halved comonomer incorporation and low-MW polymer (72 vs $123 \times 10^3 \text{ g mol}^{-1}$ - Table 2, entry 3 vs 4). Overall, the results indicate that the second $\text{C}=\text{C}$ bond in 1,5-hexadiene remarkably affects the copolymerization in terms of productivity, comonomer insertion mode and copolymer MW. These

may be related to an increased stability of cyclic intermediate in the copolymerization of 1,5-hexadiene and, on the contrary, to a faster chain termination after the last 1-hexene inserted unit.

The terpolymerization of 1,5-hexadiene with ethylene and different cyclic olefins (M2 in Scheme 4 and Table 2) was carried out at 1 atm of ethylene and E/HXD/M2 feed ratio of 1/4/0.5. **c1**/Et₂AlCl/ETA proved to be highly active in E/HXD/NB and E/HXD/ENB terpolymerizations, while the addition of bulkier DCPD was slightly detrimental to the activity. Soluble, solid terpolymers with high molecular weight (M_w above 100×10^3 g/mol), and unimodal and narrow M_w/M_n were obtained. The cyclic olefin incorporation decreases in the order NB (12.4 mol%) > ENB (8.4 mol%) > DCPD (5.8 mol%), which can be explained by steric effects. The addition of the cyclic olefin in the reaction mixture has a negative effect on 1,5-hexadiene uptake: the diene incorporation significantly decreased (MCP and VTM units in Table 2), particularly for the less steric demanding norbornene that makes 1,5-hexadiene insertion less favorable. Compared with the E/HXD copolymer, the T_g of the resulting terpolymers significantly rises because bulkier pendant cyclic olefins restrict rotational freedom to some extent. The terpolymers showed T_g s ranging between -6 and -3 °C and some of them did not show melting events since the total amount of incorporated 1,5-hexadiene and cyclic olefin is higher than 20 mol%, a composition that usually prevent crystallization (Table 2, entry 5 and 6).⁴⁰

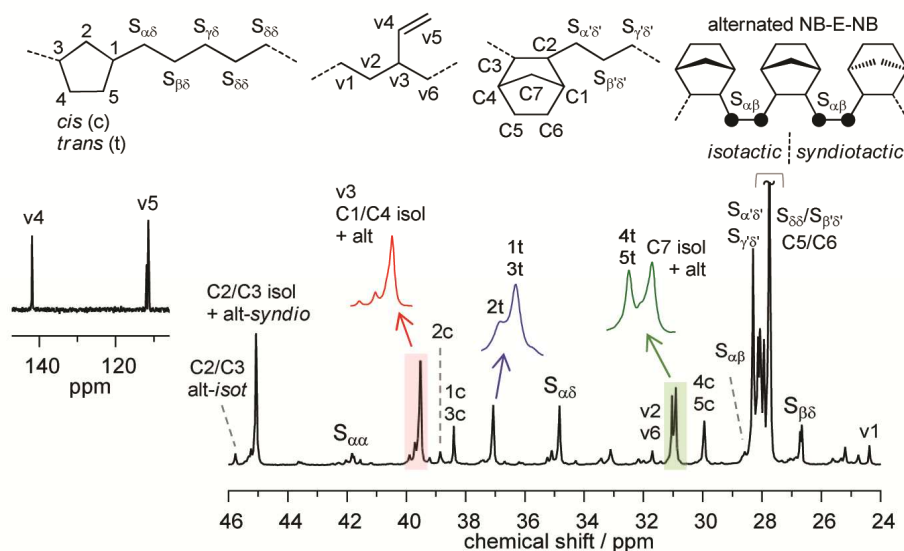
Scheme 4. Terpolymerization of ethylene with 1,5-hexadiene and different cyclic olefins (M2).



The microstructure of the resultant terpolymers was investigated by NMR. Peak assignment was carefully performed by comparison of the observed chemical shifts with those of entry **3** (Figure 3a and Table S5) and previous data by some of us.⁴¹ Figure 4 shows the ¹³C NMR spectrum of the

E/HXD/NB terpolymer along the various types of monomer enchainment fragments identified. In addition to the characteristic peaks of isolated and alternated NB units from the addition type copolymerization with *cis exo-exo* enchainment (*i.e.*, 44.7–45.7 ppm (C2/C3); 39.0–40.0 ppm (C1/C4); 30.9 ppm (C7); 27.0–29.0 ppm (C5/C6 and ethylene CH₂)), the spectrum shows resonances diagnostic of isolated MCP and VTM units from 1,2- (Scheme 1, path C) and 2,1- insertion (Scheme 1, and B) of 1,5-hexadiene, respectively. NMR analysis established that the terpolymer is formed by 78.3 mol% of ethylene, 12.4 mol% NB, and low percentages of VTM and MCP (3.2 and 6.1 mol%, respectively, proving that the 1,2-insertion of 1,5-hexadiene is favoured over 2,1-insertion).

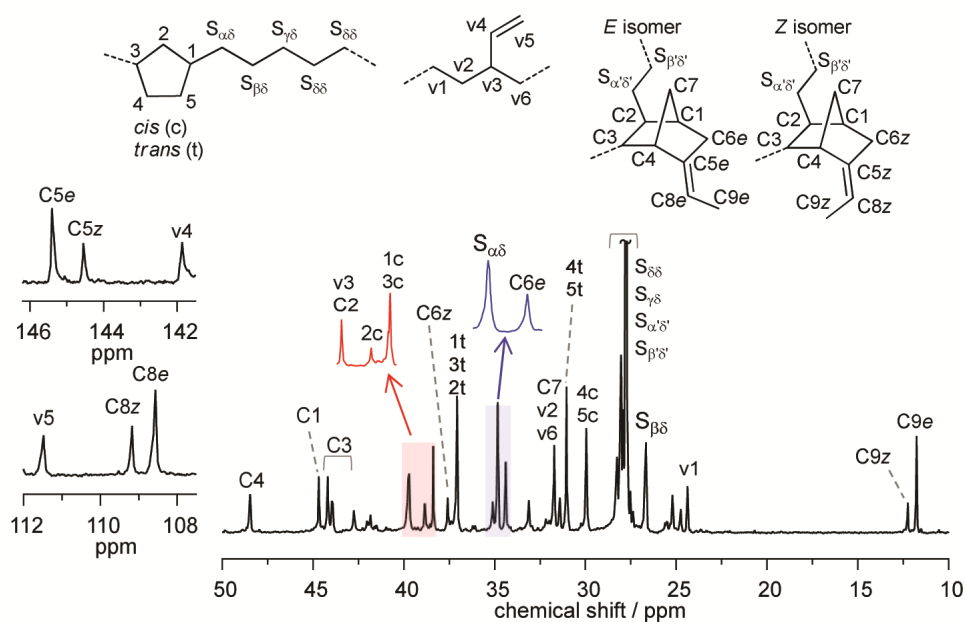
Figure 4. ¹³C NMR spectrum (in C₂D₂Cl₄ at 103 °C, reference to HDMS) of entry 5.



The ¹³C and ¹H NMR spectra of E/HXD/ENB terpolymer are shown in Figure 5 and S8, respectively. In addition to the signals ascribed to VTM and MCP units, the ¹H NMR spectrum shows signals at 5.1 and 5.3 ppm that were assigned to the ethylidene groups, while the lack of signals at about 6.0 ppm indicates that ENB inserts into the polymer chain via the enchainment of the double bond of the norbornenic ring, while ethylidene group is retained without cross-linking (Figure S8). In addition to the characteristic resonances of long methylene segments, MCP and unsaturated VTM fragments, the dominant signals in the ¹³C NMR spectrum are those due to isolated ENB units. The signals of each chemical shift region were assigned as follows: 144–146 ppm (C5), 108–109 ppm

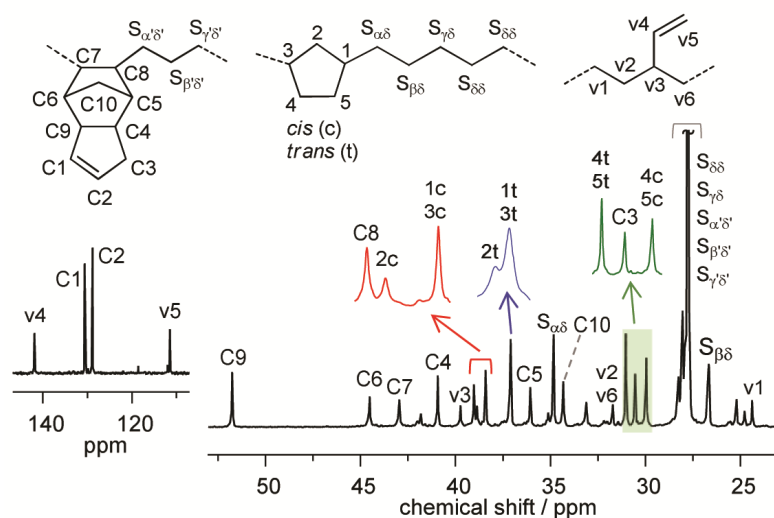
(C8), 48.4 ppm (C4), 42.0–45.0 ppm (C1/C3, with the signals ascribed to C3 located at the higher field), 37.6 ppm (C6z), 34.3 ppm (C6e), 27.0–29.0 ppm (S α' δ' , S β' δ'), 11.7 ppm (C9e) and 12.2 ppm (C9z) (Table S6).

Figure 5. ^{13}C NMR spectrum (in $\text{C}_2\text{D}_2\text{Cl}_4$ at 103 °C, reference to HDMS) of entry 6.



The ^{13}C and ^1H NMR spectra of E/HXD/DCPD terpolymer are shown in Figure 6 and S9, respectively. The peaks at 130.6 and 128.8 ppm in the ^{13}C NMR spectrum and those at 5.5 and 5.4 ppm in the ^1H NMR spectra indicate that the terpolymer contains unreacted cyclopentene units: the insertion of DCPD takes place selectively at the norbornenic ring. In addition to the intense signal at 27.7 ppm of methylene main chain segment, the dominant signals in the ^{13}C NMR spectra are those characteristics of MCP and VTM fragments, and those at 51.7 (C9), 44.5 (C6), 42.9 (C7), 40.9 (C4), 39.0 (C8), 35.9 (C5), 34.3 (C10), and 30.5 (C3) ppm assigned to isolated DCPD units (Table S7).

Figure 6. ^{13}C NMR spectrum (in $\text{C}_2\text{D}_2\text{Cl}_4$ at 103°C , reference to HDMS) of entry **8**.



To further probe the effect of the second $\text{C}=\text{C}$ bond in 1,5-hexadiene, we investigated the terpolymerization of 1-hexene with ethylene and ENB (Table 2, entry 7). The presence of 1-hexene significantly affects the activity and, more importantly, was detrimental to the terpolymer MW (51 vs $120 \times 10^3 \text{ g mol}^{-1}$ - Table 2, entry 7 vs 6) which is critical to achieve good tensile properties. This confirms the key role of 1,5-hexadiene in retarding chain termination due to a cooperative effect of the remaining $\text{C}=\text{C}$ bond.

Co- and Ter-polymerization of 1,7-Octadiene. The successful copolymerization of 1,5-hexadiene with ethylene prompted us to investigate the copolymerization of 1,7-octadiene (Table 3, entry 9 and Scheme 5). Surprisingly, **c1** catalyzed the copolymerization of 1,7-octadiene with ethylene to give a soluble, solid, semicrystalline copolymer with a good diene incorporation (9.7 mol%) and very high-MW ($M_w = 192 \times 10^3 \text{ g mol}^{-1}$). The copolymerization was stopped at the initial stage to keep low the diene conversion and to avoid intermolecular insertion (or graft addition) of vinyl moieties.

Spectroscopic characterization by NMR provided data that are fully consistent with the polymer microstructure depicted in Scheme 5. ^1H NMR spectrum indicates that the copolymer has a certain extent of terminal and internal $\text{C}=\text{C}$ bonds (Figure S10). In the ^{13}C NMR spectrum, the characteristic resonances of saturated main chain ($\text{S}_{\delta\delta}$ at 27.7 ppm), pendant hexyl groups (referred to “VHX”) at 137.3 (2B_6), 112.1 (1B_6), 35.9 ($\text{T}_{\delta\delta}$), 32.1 (6B_6), 31.7 (3B_6), 25.0 (4B_6), and 24.5 (5B_6) ppm expected

from 1,2-insertion of 1,7-octadiene, and those of linear C8 segments with an internal C=C bond (referred to “INT” – *a* at 128.5 ppm) were easily detected (Figure 7 and Table S8). NMR analysis established that the copolymer is formed by 90.3 mol% of ethylene, 8.0 mol% VHX, and 1.7 mol% INT units. The configuration of the internal double bond can also be determined: the signals at 29.9 and 27.2 ppm are ascribed to carbons attached to a *trans* internal double bond, *i.e.*, α T and β T, respectively.

Table 3. 1,7-Octadiene (OTD) Copolymerization and Terpolymerization Studies Using **c1**/Et₂AlCl/ETA.^a

entry	M1	M2	E/M1/M2 ^b	yield (g)	activity ^c	composition (mol%) ^d				$M_w^e \times 10^3$ (g/mol)	M_w/M_n^e	T_g^f (T_m) (°C)
						E	VHX	INT	M2			
9^s	OTD		1/4	0.22	322	90.3	8.0	1.7		192	3.1	(67)
10	OTD	NB	1/4/0.5	0.69	747	79.7	6.0	2.3	12.0	200	3.8	-28 (18)
11	OTD	ENB	1/4/0.5	0.55	600	85.6	7.2	1.6	5.6	196	3.3	-26 (24)
12	OTD	DCPD	1/4/0.5	0.25	269	86.6	6.9	1.6	4.9	112	2.3	-30 (44)

^a polymerization conditions: ethylene pressure, 1.01 bar; total volume, 50 mL (toluene); **c1**, 5 μ mol; Al/V = 500; ETA/V = 10; temperature, 20 °C; time, 11 min; [OTD] = 0.56 mol/L; [M2] = 0.07 mol/L;^b (co)monomer feed ratio (mol/mol) in liquid phase; ^c activity in $\text{kg}_{\text{pol}} \times (\text{mol}_V \times \text{h})^{-1}$; ^d determined by NMR; ^e determined by SEC; ^f determined by DSC (second heating); ^s time, 8 min.

Scheme 5. Copolymerization of ethylene with 1,7-octadiene by **c1**/Et₂AlCl/ETA.

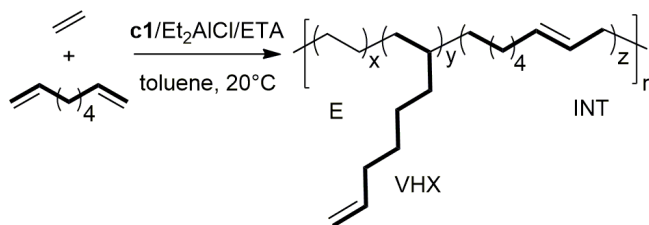
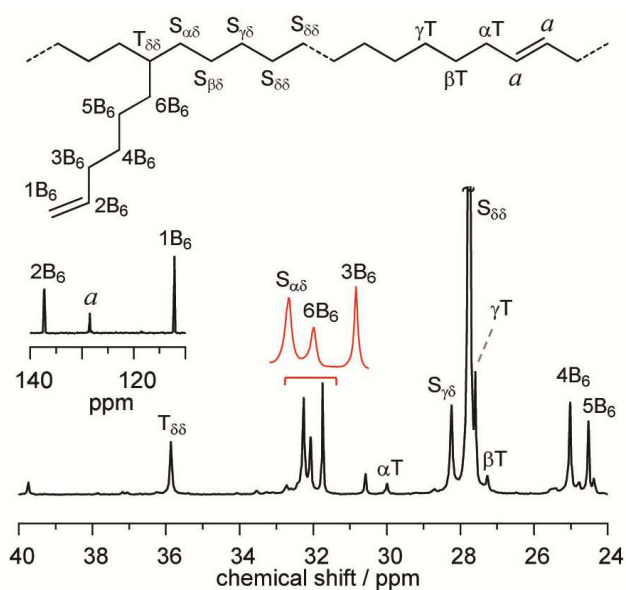
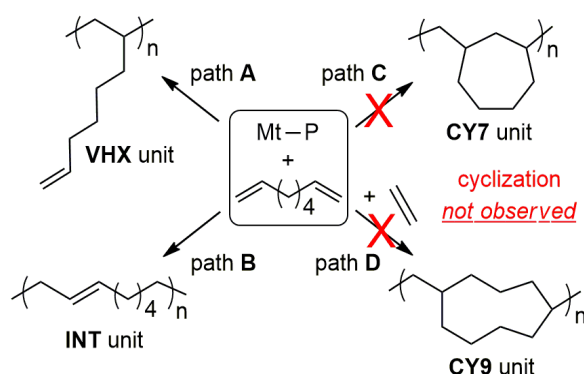


Figure 7. ^{13}C NMR spectrum (in $\text{C}_2\text{D}_2\text{Cl}_4$ at 103°C , reference to HDMS) of entry **9**.



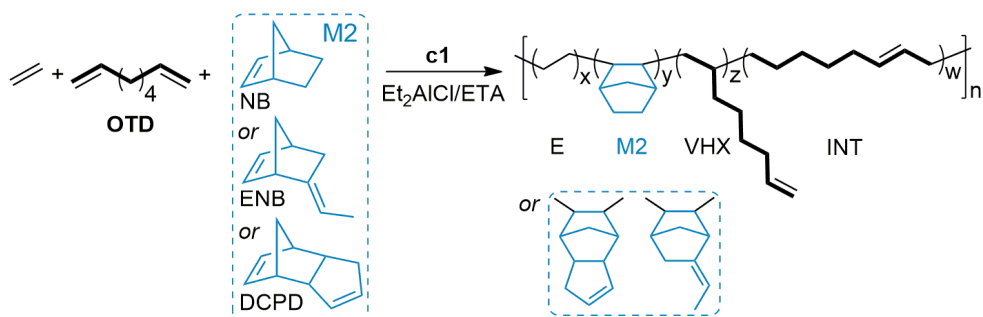
It is noteworthy that the ^{13}C NMR spectrum of entry **9** does not show any signals ascribed to cyclic units as methylene-1,3-cycloheptane fragment (referred to “CY7” in Scheme 6) and 1,5-disubstituted cyclononane unit (referred to “CY9”), expected from cyclization of penultimate insertion of 1,7-octadiene after ethylene insertion (Scheme 6, path D).⁶² It could be argued that common 1,2-insertion and double linear insertion of 1,7-octadiene (Scheme 6, path A and B, respectively) competed well against ring closure. Primary 1,2-insertion and subsequent cyclization by 1,2-insertion of the second $\text{C}=\text{C}$ bond did not occur in the case of 1,7-octadiene. This may be likely because the remaining $\text{C}=\text{C}$ bond of the last inserted 1,7-octadiene is more distant from the vanadium center than in the case of 1,5-hexadiene, making the ring closure highly disadvantaged. However, there are some reports in the literature that well describe the cyclization of 1,7-octadiene promoted by metallocenes,^{30,63,64} and carbene ligated rare-earth complexes.⁶⁵

Scheme 6. Insertion modes of 1,7-octadiene.



Terpolymerization of 1,7-octadiene with ethylene and the selected cyclic olefins were also performed (Table 3 and Scheme 7). Generally, these are much less productive than the corresponding terpolymerizations in the presence of 1,5-hexadiene, by less than one order of magnitude (entry 5 vs 10; entry 6 vs 11 and entry 8 vs 12). The observed trend may be steric in nature and well correlates with (i) the preferentially insertion mode of 1,7-octadiene and lack of cyclization selectivity, and (ii) the hypothesis first advanced, that is that with 1,5-hexadiene, cyclic intermediates play a key role in increasing the catalytic activity. The terpolymerization of 1,7-octadiene with ethylene and NB exhibited the highest activity and the highest termonomer incorporation (entry 10, NB = 12.0 mol%), while maintaining very high-MW ($M_w = 200 \times 10^3$ g/mol). By contrast, steric effects strongly limit the incorporation of bulkier DCPD (4.9 mol%) and ENB (5.6 mol%).

Scheme 7. Terpolymerization of 1,7-octadiene with ethylene and the selected M2 cyclic olefins.



Concerning the terpolymer microstructure, and particularly the enchainment of M2 cyclic olefin, ^{13}C NMR spectra showed that 1,7-octadiene terpolymers were mainly formed by isolated 2,3 *cis-exo-exo* cyclic olefin enchainment units (Figures 8–10). Both DCPD and ENB cyclic dienes insert

into the polymer via the enchainment of the double bond of the norbornenic ring, while the second C=C bond is retained. In addition to the resonances ascribed to isolated cyclic olefin units, and long methylene sequences ($S_{\delta\delta}$ at 27.7 ppm), two different kinds of enchainment 1,7-octadiene units were detected (Table S9–S11). These are: (i) pendant C6 branches with terminal C=C bond (VHX) ascribed to the common 1,2-insertion (Scheme 6, path A), and (ii) linear structures with an internal double bond (INT) due to the incorporation of both vinyl groups of 1,7-octadiene in a linear manner (Scheme 6, path B). No resonances assignable to cyclic units from the last inserted 1,7-octadiene were detected. This result further supports the lack of intramolecular coordination (ring closure) of the remaining double bond of the last inserted 1,7-octadiene unit and demonstrates that cyclization is less feasible (or at least less facile) increasing the nonconjugated diene length.

Figure 8. ^{13}C NMR spectrum (in $\text{C}_2\text{D}_2\text{Cl}_4$ at 103 °C, reference to HDMS) of entry **10**.

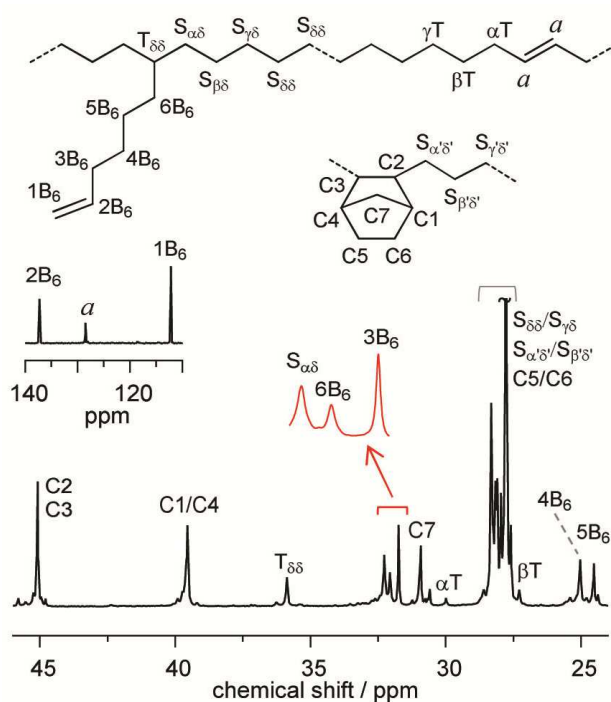


Figure 9. ^{13}C NMR spectrum (in $\text{C}_2\text{D}_2\text{Cl}_4$ at 103°C , reference to HDMS) of entry **11**.

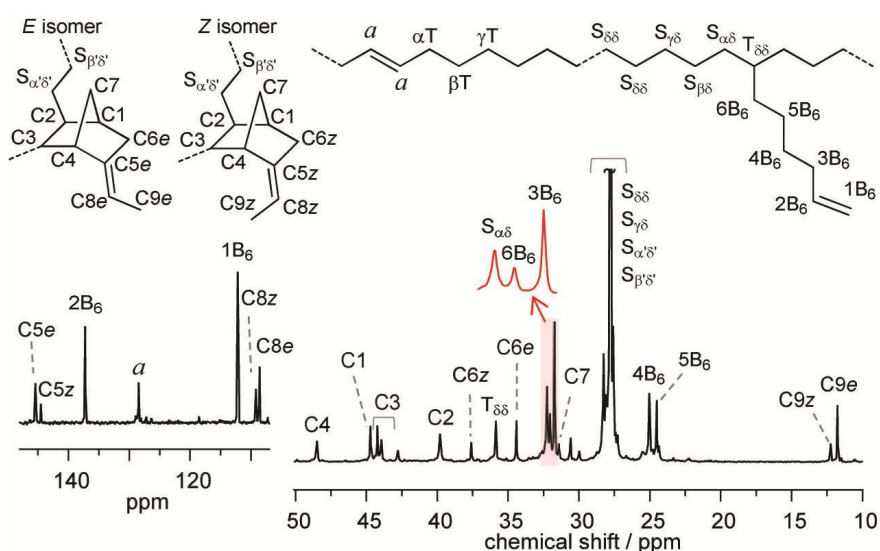
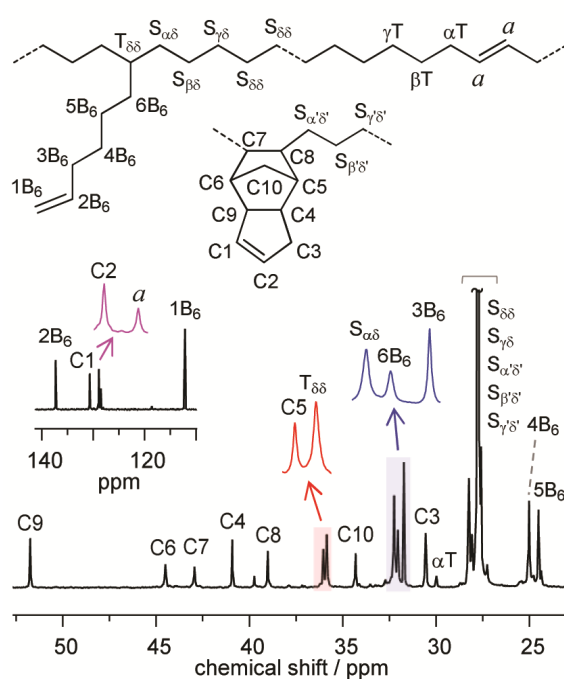


Figure 10. ^{13}C NMR spectrum (in $\text{C}_2\text{D}_2\text{Cl}_4$ at 103°C , reference to HDMS) of entry **12**.



Furthermore, it is worth to note that the presence of flexible C6 pendant groups strongly affects the T_g s. The long branches with terminal C=C bond limit the packing of the chains thus lowering the T_g up to -30°C . These olefinic branches have a more disturbing effect on thermal properties than the five-membered rings (associated with the ring closure of 1,5-hexadiene) do.

Thiol–ene Functionalization

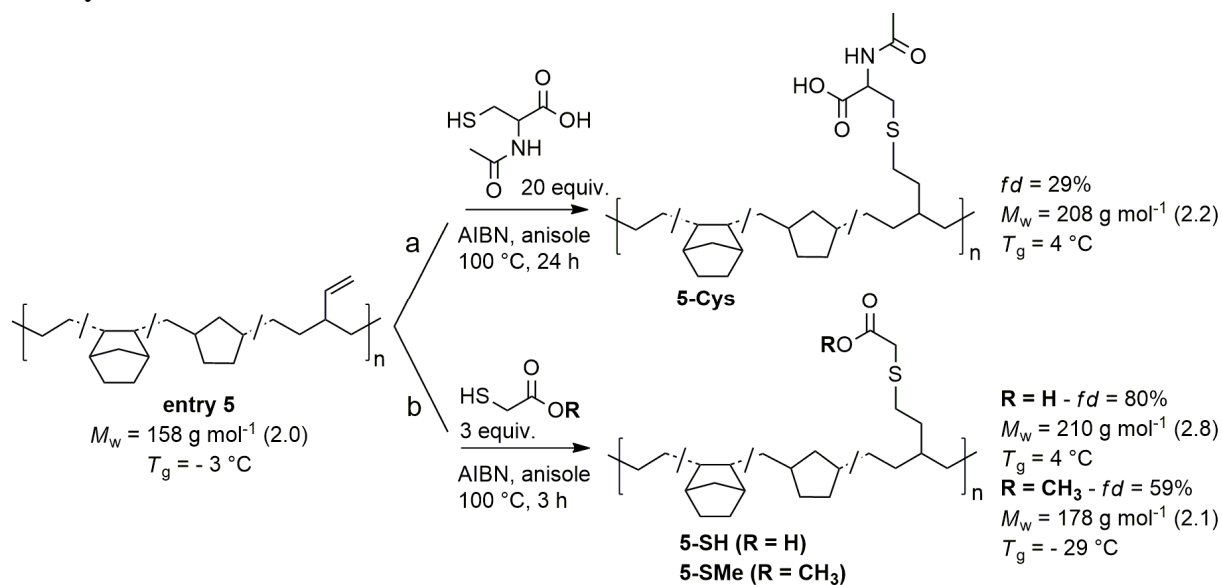
To demonstrate the application of the obtained polymers as *reactive polyolefin intermediate*, sample **5** was first subjected to thiol–ene reaction: by radical activation mediated by AIBN, the C=C bond of the VTM unit was reacted with a thiol, forming a new C–S bond (Scheme 8). Three thiols, *i.e.* thioglycolic acid, methyl thioglycolate and *N*-acetyl-L-cysteine with diverse reactivities,⁶⁶ were tested (Chart 2). The reactions proceed well in anisole at 100°C; to avoid undesirable gelation and cross-linking, the reactions were carried out in dilute conditions. The functionalization degree (*fd*) was determined by ¹H NMR by tracking characteristic signals at 4.80 ppm (two vinylic protons of the VTM unit – Figure S15–S17). The different functional polymer diversity and experimental data are given in Scheme 8.

Chart 2. Thiols used in this work.



The thiol substitution greatly impacts on the functionalization degree: the most hindered Cys brings to a 29% *fd* (Scheme 8a), SMe to 59% *fd* (Scheme 8b), while almost quantitative functionalization was obtained with SH (80% *fd*). SEC curves of all the functionalized polymers shifted to higher MW with unimodal M_w/M_n in the range 2.1–2.8 without any trace of shoulder peak. This indicates that no radical side reaction occurred. The functionalized polymers exhibited versatile thermal properties, strongly depending on the thiol substitution. For the polymer containing –OH and/or –NH functional groups (*i.e.*, **5-Cys** and **5-SH**), the T_g s raised to 4 °C. This may be likely due to the formation of hydrogen bonding among the functional groups installed on the polymer side chains, mimicking a dynamic cross-linking. Conversely, when no –OH and/or –NH functional groups are present, as in the case of **5-SMe**, the T_g shifted to lower temperatures (–29 °C).

Scheme 8. Post-polymerization functionalization of entry 5. Residual vinyl groups were not reported for clarity. The M_w/M_n is shown in brackets.



CONCLUSIONS

In summary, we report the terpolymerization of two different α,ω -dienes (*i.e.*, 1,5-hexadiene and 1,7-octadiene) with ethylene and various cyclic olefins catalyzed by a chelated imido vanadium(IV) based catalyst. A series of polyolefins with C=C bonds in the side and main chain, high-MW, sub-ambient T_g s, tunable composition, and a satisfying content of pendant vinyls can be generated with high activities. Subtle changes in the α,ω -diene size strongly influenced the monomer insertion selectivity (ring closure *vs* ring opening): 1,5-hexadiene polymers are mainly formed by methylene-1,3-cyclopentane and 3-vinyl-tetramethylene units, whereas 1,7-octadiene polymers prevail in pendant hexyl groups and linear C8 segments with an internal *trans* C=C double bond. As a proof of concept, the terpolymer of 1,5-hexadiene with ethylene and norbornene was applied to synthesize side-group functionalized polyolefins via thiol-ene chemistry. It demonstrates that the obtained unsaturated polymers are good reactive intermediates for the fabrication of versatile polar-functionalized polyolefins. Preliminary investigation of crude polymer properties revealed that they behave as elastomers and may be good toughening components (and compatibilizers) in

polyolefin blending. Further exploration of mechanical, surface, and self-healing properties of the functionalized polyolefins is underway and will be disclosed in due course.

ASSOCIATED CONTENT

Supporting Information

The Supporting Information is available free of charge on the ACS Publications website at DOI:

Experimental procedures, X-ray crystallographic details, EPR spectra, NMR assignments, polymer composition calculations, and polymer characterization data.

Accession Codes

CCDC 2106663 and 2106664 contain the supplementary crystallographic data for this paper. These data can be obtained free of charge via www.ccdc.cam.ac.uk/data_request/cif, or by emailing data_request@ccdc.cam.ac.uk, or by contacting The Cambridge Crystallographic Data Centre, 12 Union Road, Cambridge CB2 1EZ, UK; fax: +44 1223 336033.

ACKNOWLEDGEMENTS

B.P. and G.Z. thank the project “Cr4FUN –Chromium catalysis: from fundamental understanding to functional aliphatic polymers” funded by MIUR Progetti di Ricerca di Rilevante Interesse Nazionale (PRIN) Bando 2017 (20179FKR77_002) for a post-doc grant. We are grateful to Fulvia Greco, Daniele Piovani and Fabio Bertini for the acquisition of NMR spectra, SEC and DSC measurements, respectively. The CNRS is thanked for its support.

REFERENCES

- (1) Zanchin, G.; Leone G. Polyolefin thermoplastic elastomers from polymerization catalysis: Advantages, pitfalls and future challenges. *Prog. Polym. Sci.* **2021**, *113*, 101342.
- (2) Chen, C. Designing catalysts for olefin polymerization and copolymerization: beyond electronic and steric tuning. *Nat. Rev. Chem.* **2018**, *2*, 6–14.
- (3) Klosin, J.; Fontaine, P.P.; Figueroa, R. Development of Group IV Molecular Catalysts for High Temperature Ethylene- α -Olefin Copolymerization Reactions. *Acc. Chem. Res.* **2015**, *48*, 2004–2016.

- (4) Baier, M.C.; Zuideveld, M.A.; Mecking, S. Post-metallocenes in the industrial production of polyolefins. *Angew. Chem. Int. Ed.* **2014**, *53*, 9722–9744.
- (5) Zanchin, G.; Piovano, A.; Amodio, A.; De Stefano, F.; Di Girolamo, R.; Groppo, E.; Leone, G. NEt₃-Triggered Synthesis of UHMWPE Using Chromium Complexes Bearing Non-innocent Iminopyridine Ligands. *Macromolecules* **2021**, *54*, 1243–1253.
- (6) Stürzel, M.; Mihan, S.; Mülhaupt, R. From multisite polymerization catalysis to sustainable materials and all-polyolefin composites. *Chem. Rev.* **2016**, *116*, 1398–433.
- (7) Gao, Y.; Liu, W.; Zhu, S. Polyolefin thermoplastics for multiple shape and reversible shape memory. *ACS Appl. Mater. Interfaces* **2017**, *9*, 4882–4889.
- (8) Song, X.; Cao, L.; Tanaka, R.; Shiono, T.; Cai, Z. Optically Transparent Functional Polyolefin Elastomer with Excellent Mechanical and Thermal Properties. *ACS Macro Lett.* **2019**, *8*, 299–303.
- (9) Crawford, K. E.; Sita, L. R. De Novo Design of a New Class of “Hard–Soft” Amorphous, Microphase-Separated, Polyolefin Block Copolymer Thermoplastic Elastomers. *ACS Macro Lett.* **2015**, *4*, 921–925.
- (10) Tan, C.; Chen, C. Emerging palladium and nickel catalysts for copolymerization of olefins with polar monomers. *Angew. Chem. Int. Ed.* **2019**, *58*, 7192–7200.
- (11) Nakamura, A.; Anselment, T.M.J.; Claverie, J.; Goodall, B.; Jordan, R.F.; Mecking, S.; Rieger, B.; Sen, A.; van Leeuwen, P.W.N.M.; Nozaki, K.; *Ortho*-phosphinobenzenesulfonate: a superb ligand for palladium-catalyzed coordination-insertion copolymerization of polar vinyl monomers. *Acc. Chem. Res.* **2013**, *46*, 1438–1449.
- (12) Nakamura, A.; Ito, S.; Nozaki, K. Coordination-insertion copolymerization of fundamental polar monomers. *Chem. Rev.* **2009**, *109*, 5215–5244.
- (13) Zhou, G.L.; Cui, L.; Mu, H.L.; Jian, Z.B.; Custom-made polar monomers utilized in nickel and palladium promoted olefin copolymerization. *Polym. Chem.* **2021**, *12*, 3878–3892.
- (14) Dai, S.; Li, S.; Xu, G.; Chen, C. Direct synthesis of polar functionalized polyethylene thermoplastic elastomer. *Macromolecules* **2020**, *53*, 2539–4256.

- (15) Zou, C.; Chen, C. Polar-functionalized, crosslinkable, self-healing, and photoresponsive polyolefins. *Angew. Chem. Int. Ed.* **2020**, *59*, 395–402 .
- (16) Rodriguez, G.M.; Diaz-Requejo, M.M.; Perez, P.J. Metal-Catalyzed Postpolymerization Strategies for Polar Group Incorporation into Polyolefins Containing C–C, C=C, and Aromatic Rings. *Macromolecules* **2021**, *54*, 4971–4985.
- (17) Plummer, C.M.; Li, L.; Chen, Y. The post-modification of polyolefins with emerging synthetic methods. *Polym. Chem.* **2020**, *11*, 6862–6872.
- (18) Boen, N.K.; Hillmyer, M.A. Post-polymerization functionalization of polyolefins. *Chem. Soc. Rev.* **2005**, *34*, 267–275.
- (19) Williamson, J.B.; Lewis, S.E.; Johnson, R.R.; Manning, I.M.; Leibfarth, F.A. C–H functionalization of commodity polymers. *Angew. Chem. Int. Ed.* **2018**, *58*, 8654–8668.
- (20) Wang, X.Y.; Wang, Y.X.; Li, Y.S.; Pan, L. Convenient Syntheses and Versatile Functionalizations of Isotactic Polypropylene Containing Plentiful Pendant Styrene Groups with High Efficiency. *Macromolecules* **2015**, *48*, 1991–1998.
- (21) Geiselhart, C.M.; Offenloch, J.T.; Mutlu, H.; Barner-Kowollik, C. Polybutadiene Functionalization via an Efficient Avenue. *ACS Macro Lett.* **2016**, *5*, 1146–1151.
- (22) Tan, R.; Shi, Z.; Guo, F.; He, L.; Han, L.; Li, Y. The terpolymerization of ethylene and propylene with isoprene via THF-containing half-sandwich scandium catalysts: a new kind of ethylene–propylene–diene rubber and its functionalization. *Polym. Chem.* **2017**, *8*, 4651–4658.
- (23) Zanchin, G.; Leone, G.; Pierro, I.; Rapallo, A.; Porzio, W.; Bertini, F.; Ricci, G. Addition Oligomerization of Dicyclopentadiene: Reactivity of *Endo* and *Exo* Isomers and Postmodification. *Macromol. Chem. Phys.* **2017**, *218*, 1600602.
- (24) Li, L.; Li, S.; Cui, D. Highly *Cis*-1,4-Selective Living Polymerization of 3-Methylenehepta-1,6-diene and Its Subsequent Thiol–Ene Reaction: An Efficient Approach to Functionalized Diene-Based Elastomer. *Macromolecules* **2016**, *49*, 1242–1251.

- (25) Xu, J.; Boyer, C. Visible Light Photocatalytic Thiol–Ene Reaction: An Elegant Approach for Fast Polymer Postfunctionalization and Step-Growth Polymerization. *Macromolecules* **2015**, *48*, 520–529.
- (26) Osakada, K.; Takeuchi, D. Coordination Polymerization of Dienes, Allenes, and Methylenecycloalkanes. In: Polymer Synthesis. *Advances in Polymer Science*, **2004**, vol. 171. Springer, Berlin, Heidelberg.
- (27) Pasini, D.; Takeuchi, D. Cyclopolymerizations: Synthetic Tools for the Precision Synthesis of Macromolecular Architectures. *Chem. Rev.* **2018**, *118*, 8983–9057.
- (28) Hustad, P.D.; Coates, G.W. Insertion/Isomerization Polymerization of 1,5-Hexadiene: Synthesis of Functional Propylene Copolymers and Block Copolymers. *J. Am. Chem. Soc.* **2002**, *124*, 11578–11579.
- (29) Han, S.; Yao, E.; Quin, W.; Zhang, S.; Ma, Y. Binuclear Heteroligated titanium Catalyst Based on Phenoxyimine Ligands: Synthesis, Characterization, and Ethylene Copolymerization. *Macromolecules* **2012**, *45*, 4054–4059.
- (30) Naga, N.; Imanishi, Y. Copolymerization of Ethylene and 1,7-Octadiene, 1,9-Decadiene with Zirconocene Catalysts. *Macromol. Chem. Phys.* **2002**, *203*, 2155–2162.
- (31) Shi, X.; Wang, Y.; Liu, J.; Cui, D.; Men, Y.; Li, Y. Stereospecific Cyclopolymerization on of α,ω -Diolefins by Pyridylamidohafnium Catalyst with the Highest Activity. *Macromolecules* **2011**, *44*, 1062–1065.
- (32) Takeuchi, D.; Matsuura, R.; Osakada, K. Copolymerization of Hepta-1,6-diene with Ethylene Catalyzed by Cobalt Complexes. *Makromol. Rapid Commun.* **2008**, *29*, 1932–1936.
- (33) Guo, F.; Nishiura, M.; Koshino, H.; Hou, Z. Cycloolefin polymerization of 1,6-heptadiene with ethylene and styrene catalyzed by a THF-free half-sandwich scandium complex. *Macromolecules* **2011**, *44*, 2400–2403.
- (34) Guo, F.; Nishiura, M.; Koshino, H.; Hou, Z. Scandium-Catalyzed Cycloolefin polymerization of 1,5-Hexadiene with Styrene and Ethylene: Efficient Synthesis of Cycloolefins Containing

Syndiotactic Styrene–Styrene Sequences and Methylene-1,3-cyclopentane Units. *Macromolecules* **2011**, *44*, 6335–6344.

(35) Apisuk, W.; Nomura, K. Efficient Terpolymerization of Ethylene and Styrene with 1,7-Octadiene by Aryloxo Modified Half-Titanocenes–Cocatalyst Systems: Efficient Introduction of the Reactive Functionality. *Makromol. Chem. Phys.* **2014**, *215*, 1785–1791.

(36) Faisca Phillips, A.M.; Suo, H.; Guedes da Silva, M.C.; Pombeiro, A.J.L.; Sun, W.H. Recent developments in vanadium-catalyzed olefin coordination polymerization. *Coord. Chem. Rev.* **2020**, *416*, 213332.

(37) Doi, Y.; Tokuhira, N.; Soga, K. Synthesis and structure of a “living” copolymer of propylene and 1,5-hexadiene. *Makromol. Chem.* **1989**, *190*, 643–651.

(38) Doi, Y.; Tokuhira, N.; Soga, K. Polymerization of Diolefins by a Soluble Vanadium-Based Catalyst. *Kobunshi Ronbunshu* **1989**, *46*, 215–222.

(39) Zanchin, G.; Bertini, F.; Vendier, L.; Ricci, G.; Lorber, C.; Leone, G. Copolymerization of ethylene with propylene and higher α -olefins catalyzed by (imido)vanadium(IV) dichloride complexes. *Polym. Chem.* **2019**, *10*, 6200–6216.

(40) Leone, G.; Zanchin, G.; Di Girolamo, R.; De Stefano, F.; Lorber, C.; De Rosa, C.; Ricci, G.; Bertini, F.; Semibatch Terpolymerization of Ethylene, Propylene, and 5-Ethylidene-2-norbornene: Heterogeneous High-Ethylene EPDM Thermoplastic Elastomers. *Macromolecules* **2020**, *53*, 5881–5894.

(41) Zanchin, G.; Vendier, L.; Pierro, I.; Bertini, F.; Ricci, G.; Lorber, C.; Leone, G. Homo- and Co-Polymerization of Ethylene with Cyclic Olefins Catalyzed by Phosphine Adducts of (Imido)-vanadium(IV) Complexes. *Organometallics* **2018**, *37*, 3181–3195.

(42) Zanchin, G.; Pierro, I.; Parisini, E.; Marti-Rujas, J.; Ricci, G.; Leone, G. Synthesis, structure and behavior of vanadium(III) diphosphine complexes in the homo- and co-polymerization of ethylene with norbornene: the ligand donor strength and bite angle make the difference. *J. Organomet. Chem.* **2018**, *861*, 142–150.

- (43) Nguyen, V. H.; Vendier, L.; Etienne, M.; Despagnet-Ayoub, E.; Breuil, P.-A. R.; Magna, L.; Proriol, D.; Olivier-Bourbigou, H.; Lorber, C. Titanium–Imido Complexes with Pendant Groups – Synthesis, Characterization, and Evaluation of Their Role as Precatalysts for Ethylene Polymerization. *Eur. J. Inorg. Chem.* **2012**, *1*, 97–111.
- (44) Adams, N.; Bigmore, H. R.; Blundell, T. L.; Boyd, C. L.; Dubberley, S. R.; Sealey, A. J.; Cowley, A. R.; Skinner, M. E. G.; Mountford, P. New titanium imido synthons: Syntheses and supramolecular structures. *Inorg. Chem.* **2005**, *44*, 2882–2894.
- (45) Lorber, C.; Choukroun, R.; Donnadiou, B. Synthesis and Crystal Structure of Unprecedented Phosphine Adducts of d¹-Aryl Imido–Vanadium(IV) Complexes. *Inorg. Chem.* **2003**, *42*, 673–675.
- (46) Blake, A. J.; Collier, P. E.; Dunn, S.C.; Li, W.S.; Mountford, P.; Shishkin, O.V. Synthesis and imido-group exchange reactions of tert-butylimidotitanium complexes. *Dalton Trans.* **1997**, 1549–1558.
- (47) Selby, J.D.; Manley, C.D.; Schwarz, A.D.; Clot, E.; Mountford, P. Titanium Hydrazides Supported by Diamide-Amine and Related Ligands: A Combined Experimental and DFT Study. *Organometallics* **2008**, *27*, 6479–6494.
- (48) Lorber, C.; Donnadiou, B.; Choukroun, R. Synthesis and X-ray characterization of a monomeric Cp-free d¹-imido–vanadium(IV) complex. *Dalton Trans.* **2000**, 4497–4498.
- (49) Lorber, C.; Choukroun, R.; Donnadiou, B. Synthesis and Structure of a Series of New d¹-Aryl Imido–Vanadium(IV) Complexes Stabilized by N-Donor Ligands. *Inorg. Chem.* **2002**, *41*, 4216–4226.
- (50) Lorber, C.; Choukroun, R.; Vendier, L. Hydroamination of Alkynes Catalyzed by Imido Complexes of Titanium and Vanadium. *Organometallics*, **2004**, *23*, 1845–1850.
- (51) Lorber, C.; Choukroun, R.; Vendier, L. A General and Facile One-Step Synthesis of Imido–Titanium(IV) Complexes: Application to the Synthesis of Compounds Containing Functionalized or Chiral Imido Ligands and Bimetallic Diimido Architectures. *Eur. J. Inorg. Chem.* **2006**, *22*, 4503–4518.

- (52) Lorber, C.; Choukroun, R.; Vendier, L. Reaction of *p*-Toluenesulfonylamide and $M(\text{NMe}_2)_4$ ($M = \text{Ti, V}$): Generation of Electron-Deficient Imido Complexes of Early Transition Metals. *Inorg. Chem.* **2007**, *46*, 3192–3202.
- (53) Lorber, C.; Vendier, L. Routes to New *N*-Heterocyclic Carbene Titanium(IV) Imido Complexes. *Organometallics* **2008**, *27*, 2774–2783.
- (54) Lorber, C.; Vendier, L. Synthesis and structure of early transition metal NHC complexes. *Dalton Trans.* **2009**, 6972–6984.
- (55) Lorber, C.; Vendier, L. Imido–Titanium/Molybdenum Heterobimetallic Systems. Switching from η^6 -Arene to Fischer-Type Aminocarbene Complexes by Tuning Reactivity Conditions. *Organometallics* **2010**, *29*, 1127–1136.
- (56) Addison, A. W.; Rao, T. N.; Reedijk, J.; van Rijn, J. V. Synthesis, structure, and spectroscopic properties of copper(II) compounds containing nitrogen–sulphur donor ligands; the crystal and molecular structure of aqua[1,7-bis(*N*-methylbenzimidazol-2'-yl)-2,6-dithiaheptane]copper(II) perchlorate. *J. Chem. Soc., Dalton Trans.* **1984**, 1349–1356.
- (57) Leone, G.; Pierro, I.; Zanchin, G.; Forni, A.; Bertini, F.; Rapallo, A.; Ricci, G. Vanadium(III)–catalyzed copolymerization of ethylene with norbornene: Microstructure at tetrad level and reactivity ratios. *J. Mol. Cat. A: Chem.* **2016**, *424*, 220–231.
- (58) Nomura, K.; Takemoto, A.; Hatanaka, Y.; Okumura, H.; Fujiki, M. M. Hasegawa, K. Polymerization of 1,5-hexadiene by Half-Titanocenes–MAO Catalyst Systems: Factors Affecting the Selectivity for the Favored repeated 1,2-Insertion. *Macromolecules* **2006**, *39*, 4009–4017.
- (59) Hou, W.; Zhang, D.; Camacho-Fernandez, M.A.; Zhang, Y.; Liu, G.; Tang, Y.; Guan, Z.; Huang, Z. Double-Linear Insertion Mode of α,ω -Dienes Enabled by Thiol-imino-quinoline Iron Catalyst. *ACS Catal.* **2020**, *10*, 15092–15103.
- (60) Pierro, I.; Zanchin, G.; Parisini, E.; Martí-Rujas, J.; Canetti, M.; Ricci, G.; Bertini, F.; Leone, G. Chain-Walking Polymerization of α -Olefins by α -Diimine Ni(II) Complexes: Effect of Reducing the

Steric Hindrance of *Ortho*- and *Para*-Aryl Substituents on the Catalytic Behavior, Monomer Enchainment, and Polymer Properties. *Macromolecules* **2018**, *51*, 801–814.

(61) Leone, G.; Mauri, M.; Losio, S.; Bertini, F.; Ricci, G.; Porri, L. Copolymerization of ethylene with α -olefins and cyclic olefins catalyzed by a Ti(IV) diisopropoxy complex bearing a tridentate [O⁻,S,O⁻]-type bis(phenolato) ligand. *Polym. Chem.* **2014**, *5*, 3412–3423.

(62) Naga, N.; Toyota, A. Unique Insertion of 1,7-Octadiene in Copolymerization with Ethylene by a Constrained-Geometry Catalyst. *Macromol. Rapid. Commun.* **2004**, *25*, 1623–1627.

(63) Naga, N.; Shiono, T.; Ikeda, T. Cyclopolymerization of 1,7-octadiene with metallocene/methylaluminoxane. *Makromol. Chem. Phys.* **1999**, *200*, 1466–1472.

(64) Nomura, K.; Liu, J.; Fujiki, M.; Takemoto, A. Facile, Efficient Functionalization of Polyolefins via Controlled Incorporation of Terminal Olefins by Repeated 1,7-Octadiene Insertion. *J. Am. Chem. Soc.* **2007**, *129*, 14170–14171.

(65) Pan, Y.; Zhao, A.; Li, Y.; Li, W.; So, Y.M.; Yan, X.; He, G. Bis(oxazoline)-derived N-heterocyclic carbene ligated rare-earth metal complexes: synthesis, structure, and polymerization performance. *Dalton Trans.* **2018**, *47*, 13815–13823.

(66) Hong, M.; Liu, S.R.; Li, B.X.; Li, Y.S. Application of Thiol-ene Click Chemistry to Preparation of Functional Polyethylene with High Molecular Weight and High Polar Group Content: Influence of Thiol Structure and Vinyl Type in Reactivity. *J. Polym. Sci. Part A: Polym. Chem.* **2012**, *50*, 2499–2506.